Uncertainty evaluation for three-dimensional scanning electron microscope reconstructions based on the stereo-pair technique

Meas. Sci. Technol. **22** (2011) 035103 (11pp) doi:10.1088/0957-0233/22/3/035103

Uncertainty evaluation for three-dimensional scanning electron microscope reconstructions based on the stereo-pair technique

L Carli[1], G Genta[2], A Cantatore[1], G Barbato[2], L De Chiffre[1] and R Levi[2]

[1] Department of Mechanical Engineering, Technical University of Denmark (DTU), Produktionstorvet, Building 425, 2800 Kongens Lyngby, Denmark
[2] Department of Production Systems and Business Economics, Politecnico di Torino, Corso Duca degli Abruzzi 24, 10129 Torino, Italy

E-mail: loca@mek.dtu.dk and gianfranco.genta@polito.it

Received 13 September 2010, in final form 3 December 2010
Published 1 February 2011
Online at stacks.iop.org/MST/22/035103

Abstract
3D-SEM is a method, based on the stereophotogrammetry technique, which obtains three-dimensional topographic reconstructions starting typically from two SEM images, called the stereo-pair. In this work, a theoretical uncertainty evaluation of the stereo-pair technique, according to GUM (*Guide to the Expression of Uncertainty in Measurement*), was carried out, considering 3D-SEM reconstructions of a wire gauge with a reference diameter of 250 μm. Starting from the more commonly used tilting strategy, one based on the item rotation inside the SEM chamber was also adopted. The latter enables multiple-view reconstructions of the cylindrical item under consideration. Uncertainty evaluation was performed starting from a modified version of the Piazzesi equation, enabling the calculation of the z-coordinate from a given stereo-pair. The metrological characteristics of each input variable have been taken into account and a SEM stage calibration has been performed. Uncertainty tables for the cases of tilt and rotation were then produced, leading to the calculation of expanded uncertainty. For the case of rotation, the largest uncertainty contribution resulted to be the rotational angle; however, for the case of tilt it resulted to be the pixel size. A relative expanded uncertainty equal to 5% and 4% was obtained for the case of rotation and tilt, respectively.

Keywords: measurement uncertainty, multiple-view strategy, SEM, stereo-pair technique, surface reconstruction, wire gauge

1. Introduction and case study

Scanning electron microscopy (SEM) has some unique properties that, combined together, are not matched by any other microscopy technique. SEM is a multi-scale technique which allows image ranges from 1 mm^2 down to 1 μm^2 with an ultimate resolution as small as about 1 nm (at high magnifications), comparable to scanning probe microscopes (SPM). Other unique capabilities are the large depth of field and the long working distance usable which allow development of measuring strategies based on multiple positioning (Marinello *et al* 2008a). In particular SEM seems to be a very promising technique with respect to measuring surfaces having high aspect ratios. Many application areas are foreseen specifically for this technique such as the semiconductor industry, life sciences, materials research and many industrial fields related to nanotechnology. Nevertheless, many developments are still needed in order to transform SEM into a technique where the complete topography can be determined by a truly 3D characterization of the surface, developing metrologically correct techniques and producing traceable measurement results. In fact SEM images

are purely two dimensional, as they are built up by sensing intensity variations revealed when an electron beam is scanned over the specimen surface (secondary emission detection). A possible way to overcome these limitations is to use SEM in conjunction with image processing from stereographs (Sato 1990). This method, called the 3D-SEM technique, is based on photogrammetry and allows reconstructing the third dimension of surface features. The stereophotogrammetry technique has been extensively studied (Boyde 1973, Hillmann 1980, Kolednik 1981, Schubert *et al* 1996, Scherer 2002) starting from the theoretical description, applied to SEM, given by Piazzesi (1973). Some other authors (Bariani 2005, Marinello *et al* 2008b) have already discussed the influence of various factors on reconstruction accuracy divided into two main classes of variables: the first one related to the measurement operation and the instrument setup and the second concerning the quality of scanned images and software reconstruction. This technique has been widely used also at the authors' department in the past few years (Bariani *et al* 2005, Marinello *et al* 2008a). In the first case an uncertainty evaluation of the stereo-pair technique was performed using calibrated gauge-blocks forming steps of different heights and by the use of two ISO 5436 type C2 roughness standards, while in the second case a newly developed step-height was adopted. In both cases plane items were used enabling uncertainty evaluation when measuring different heights using the 3D-SEM technique. Anyhow, this measuring procedure still remains valid also in the case of cylindrical items where the object can be positioned and fixed horizontally to the SEM stage to perform eucentric tilting. Multiple views of the item can be acquired, at different tilt angles, to be later on used to form stereo-pairs or stereo-triplets enabling 3D reconstructions using commercial software. Another possibility is, instead, to position and clamp the cylindrical object vertically on the SEM stage, and then to tilt it by 90°. In this case the multiple views of the item can be obtained not through a tilt, but by performing rotations along the main axis of the cylinder. The main advantage of this second possibility is the fact that multiple views of the complete geometry of the object can be acquired, while in the case of tilting, only images of a limited portion of the item can be obtained. Figure 1 shows the moving stage of the SEM Inspect 'S' employed in this work where all the possible spatial movements, translations along the *x*-, *y*- and *z*-axis, *yz* tilt and rotation around the *z*-axis are also indicated. Therefore five degrees of freedom (d.o.f.) are available for positioning the item in the desired position.

In this work, a theoretical uncertainty evaluation of stereo-pair reconstructions was carried out, concerning both tilting and rotation strategies. As a case study, a wire gauge from TESA Technology, with an external calibrated diameter of 250 μm, as a cylindrical item (see figure 2) was considered.

A minor problem arises when the item rotation measuring technique is chosen, as the stage can be tilted up to maximum 78°, meaning that the item cannot be perfectly positioned parallel to the stage. This can be seen from figure 3 where an example of the cylindrical item clamped to the stage and tilted by 78°on the SEM stage is shown.

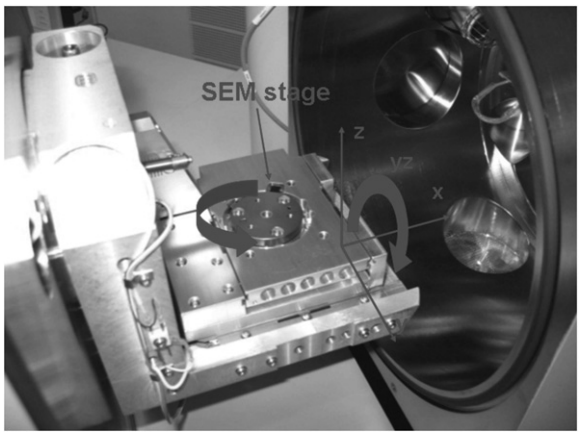

Figure 1. Image showing the SEM Inspect 'S' stage, from FEI company, enabling translations along the *x*-, *y*- and *z*-axis, *yz* tilt and rotation around the *z*-axis, meaning that five d.o.f. are available for positioning the item in the desired position.

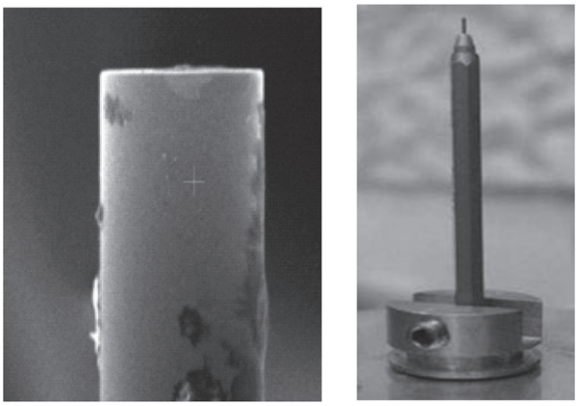

(*a*) (*b*)

Figure 2. Low magnification SEM image (*a*) of a TESA wire gauge, with an external calibrated diameter of 250 μm, and wire gauge clamping on the SEM stage (*b*).

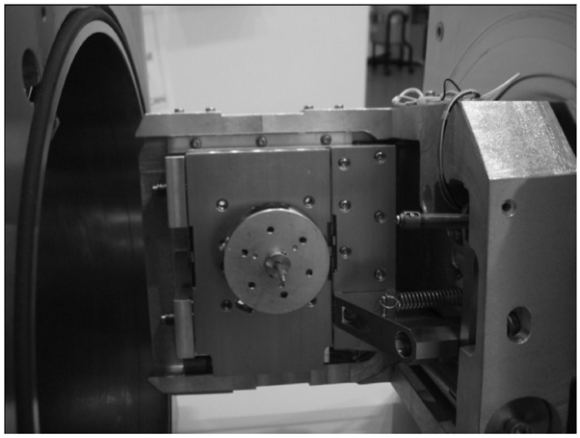

Figure 3. Image showing the reference wire gauge, clamped to the stage and tilted to the maximum allowed amount, 78°, on the SEM stage.

By knowing the wire gauge external diameter size, which is 250 μm, the optimum magnification can be calculated,

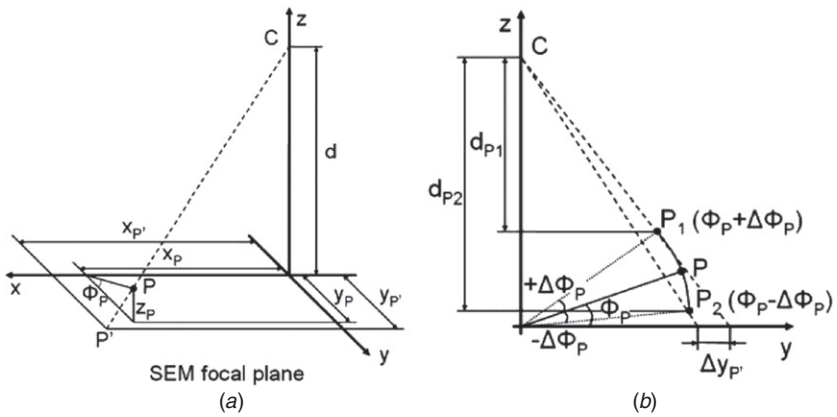

Figure 4. Geometrical definitions relative to a point P on the specimen surface. The working distance d is not shown to scale (under scaled) for ease of interpretation (Marinello *et al* 2008b).

based on the desired field of view (FOV). This requirement results in M values lower than or equal to 1000× for the SEM used in this work. The working distance value is not decided *a priori* by the operator, but it results from the adjustment of the cylindrical item which should be positioned as close as possible to the objective lenses. The working distance nominal values were derived from the SEM images of the wire gauge as performed by Carli (2010). The tilt or rotational angle between two images forming a stereo-pair can instead be chosen by the operation based on the required measuring strategy. For the choice of the optimum angle value, some considerations may be taken into account. Smaller tilt angles yield reconstructions with steeper slopes and they are suitable for higher specimens, while larger tilt angles provide better vertical resolutions and they are generally used with flat specimens. In a previous work (Carli *et al* 2009), the influence of the rotational angle on the 3D-SEM reconstruction quality was discussed.

2. Theoretical principles of the stereo-pair technique

To produce a stereoscopic reconstruction, a specimen is imaged in the SEM acquiring two images, the stereo-pair, by scanning the same area under two different perspectives, achieved by eucentric tilt of the sample. Surface features of different heights on the specimen surface differ in their lateral displacement in the two images. The disparities between the projections of the surface features in the two images are measured to derive quantitative surface topography. This is the so-called parallax movement, which is the shift of a feature from its location in the first image to the new location in the second image. For a proper measurement of the parallax it is of paramount importance to be able to successfully calculate the correct matching of single surface features in the two images. The image-matching problem mainly encompasses automatic identification in the stereo-pair of homologous points, representative of corresponding features. Nowadays this procedure is performed using commercial software where the stereo-matching is done using an area-based or a feature-based method (Scharstein and Szeliski 2002). In most SEMs, it is possible to take the two different stereo viewpoints by tilting the specimen about a horizontal axis x. Assuming that the surface region on the x-axis is brought into focus, the SEM focal plane then coincides with the reference x-, y-coordinate plane. The stereo-pair technique may be defined using the geometrical definitions given in figure 4.

With reference to figure 4(a), P is a point elevated with respect to the reference plane by an unknown amount z_P and with unknown lateral coordinates x_P and y_P; the projection of point P on the reference plane is denoted as P'. A phase angle φ_P describing the surface angular position for the given point P and relative to the tilt can be defined as sketched in figure 4(a). The consequences of eucentric tilting are shown in figure 4(b).

When rotations of $-\Delta\varphi$ and $+\Delta\varphi$ are imposed on the specimen, point P projections on the reference plane undergo a parallax Δy. Piazzesi (1973) provided a model for deriving surface topography from eucentric stereo-pairs, exploiting the physical P coordinates (ξ, η, z). Fixing the constraint $d_1 = d_2 = d$, i.e. constant working distance between the two images (Bariani 2005), the model becomes

$$\begin{cases} z = \dfrac{(y_1 - y_2)\cos\Delta\varphi + \frac{2y_1y_2}{d}\sin\Delta\varphi}{\left(1 + \frac{y_1y_2}{d^2}\right)\sin 2\Delta\varphi + \frac{y_1 - y_2}{d}\cos 2\Delta\varphi} \\ \xi = \dfrac{2d - 2z\cos\Delta\varphi}{\frac{d}{x_1} + \frac{d}{x_2}} \\ \eta = \dfrac{(y_1 + y_2)(z\cos\Delta\varphi - d)}{(y_1 - y_2)\sin\Delta\varphi - 2d\cos\Delta\varphi}, \end{cases} \tag{1}$$

where the indices 1 and 2 refer respectively to the first image (tilted by an amount $-\Delta\varphi$) and the second image (tilted by an amount $+\Delta\varphi$) being used for the calculation.

Equation (1) can be written in a different form based on the following considerations. The distance between two points in a digital picture is given by the number[3] of pixels n counted between the two points multiplied by the single pixel dimension (pixel size) p; therefore it holds that $y_1 = n_1 p$

[3] The number of pixels n is not necessarily an integer, depending on possible subpixeling.

and $y_2 = n_2 p$. It follows that the Piazzesi equation for the z-coordinate becomes

$$z = \frac{p(n_1 - n_2)\cos\Delta\varphi + \frac{2p^2 n_1 n_2}{d}\sin\Delta\varphi}{\left(1 + \frac{p^2 n_1 n_2}{d^2}\right)\sin 2\Delta\varphi + p\frac{n_1 - n_2}{d}\cos 2\Delta\varphi}. \quad (2)$$

A theoretical uncertainty evaluation, according to GUM (*Guide to the Expression of Uncertainty in Measurement*, JCGM 100:2008), has been performed starting from equation (2), thus considering p, n_1, n_2, d and $\Delta\varphi$ as independent variables. It is subsequent to a preliminary evaluation given in Genta (2010). It has been checked that a linear approximation of the measurement function is acceptable within the range of variation of input quantities. On the other hand, the hypothesis of non-correlation among input quantities is supported by the following considerations. The pixel size p and working distance d are instrument parameters which can be reasonably assumed constant, while the tilt angle $\Delta\varphi$ is a process parameter; therefore these variables are not correlated.

In the measurement process $\Delta\varphi$ is also constant, so, for a given value of z, pixel numbers n_1 and n_2 remain constant. In particular, the last two variables are, in principle, not correlated because there is no reason to suppose that for n_1 and n_2 nominally constant, a variation of the n_1 measured value involves a variation of the n_2 measured value of the same or the opposite sign. In fact, each of the mentioned variables is affected by random effects[4]. In conclusion, the presence of correlation among variables seems to be unlikely.

In particular, the tilt angle (or, similarly, rotational angle) $\Delta\varphi$ is chosen *a priori* before performing the reconstructions, while the working distance d can be read on the screen when SEM measurements are carried out. The pixel size p is linked to instrument settings, mainly to magnification level (Carli *et al* 2010). Pixel numbers n_1 and n_2 are instead directly read on the images composing the stereo-pair as previously described.

The metrological characteristics of each input variable (p, n_1, n_2, d and $\Delta\varphi$) have to be taken into account. In fact, ISO/IEC 17025:2005 deals with a concept of 'measurement complex' (clause 5.1.1) stressing the important effect on the measurement uncertainty of all the factors involved (clause 5.4.6.3), that is measuring instrument, operators, working conditions and measurand. Note that uncertainty factors related to the instrument are usually given by bias, repeatability and resolution, while other factors can be determined through a reproducibility evaluation. Detailed definitions of these terms are given in VIM (*International Vocabulary of Metrology*, JCGM 200:2008).

Therefore, in principle, reproducibility comprises repeatability and resolution; however, in a few cases, resolution is the worst characteristic, therefore it shall be taken into account. On the other hand, when it falls well below 50% of reproducibility, it may be reasonably neglected as its contribution in the quadratic composition becomes marginal.

[4] Although there exists a deterministic relationship between the variables, this does not necessarily imply a correlation between the measurement results, since the deterministic part of the variability may be negligible compared with random contributions.

The theoretical uncertainty evaluation was carried out considering two cases, tilt and rotation, to allow for a comparison between these two measuring strategies. Moreover, some calibration operations were necessary, since no calibration certificate or any other information was available stating SEM stage performances.

3. Evaluation of main uncertainty contributions

3.1. Pixel size

3.1.1. Bias evaluation. The pixel size p has been calibrated through a TGT1 silicon grating from NT-MDT Company, intended for SPM calibration. The grating consists of an array of sharp tips with a period of 3.00 ± 0.05 μm and a diagonal period of 2.12 μm as declared by the producer (a 3D rendering of TGT1 is given in figure 5).

This calibration procedure was carried out at fixed values of the main instrument settings (i.e. accelerating voltage $HV = 10$ kV and spot size $SS = 4$ nm) and of the working distance ($d = 7.3$ mm). The whole range of magnification M in the measurement conditions has been explored. In particular 23 SEM images of the calibrated artefact were acquired to allow for pixel size calculation starting from the calibrated value of the diagonal period. Images were taken for increasing values of M. Among the 23 experiments, a total of five replications were performed both at $M = 1000\times$ and at $M = 10\,000\times$ to enable reproducibility evaluation. A graph was produced (see figure 6) where the empirical relation (regression dotted curve) between the pixel size p and magnification M was calculated from 15 experiments (replications were not considered). The goodness of fit of the empirical relation is confirmed by the standard deviation of residuals, which results to be 5×10^{-4} μm/pixel. It also means that the uncertainty of the model is negligible. On a digital SEM, the picture element is the region on the sample surface where the beam interacts. The magnification can be defined as the ratio between the size of the pixel element in the image domain and the corresponding picture element dimension. In other words, the magnification is in inverse proportion to the pixel size (Goodhew *et al* 2001). For this reason the mathematical pixel size formulation calculated from the graph of figure 6 can be approximated by the hyperbola $p = 293.2/M$.

The bias to be considered in this case is the one derived from the artefact, calibrated with a declared period variability of 0.05 μm. In the evaluation, just to be on the safe side, this variability, corresponding to a relative value of 1.6%, is totally attributed to bias error (that is the most severe condition). For this contribution, a uniform distribution has been assumed. For magnifications equal to $800\times$ (i.e. 800 times) and $1000\times$, the pixel size results equal respectively to 0.366 and 0.293 μm/pixel. Therefore, the bias is equal to about 5.9×10^{-3} and 4.7×10^{-3} μm/pixel, respectively.

3.1.2. Reproducibility evaluation. Fixing the magnification to $1000\times$, the standard deviation of the five replicated measurements is equal to 6.2×10^{-4} μm/pixel. For

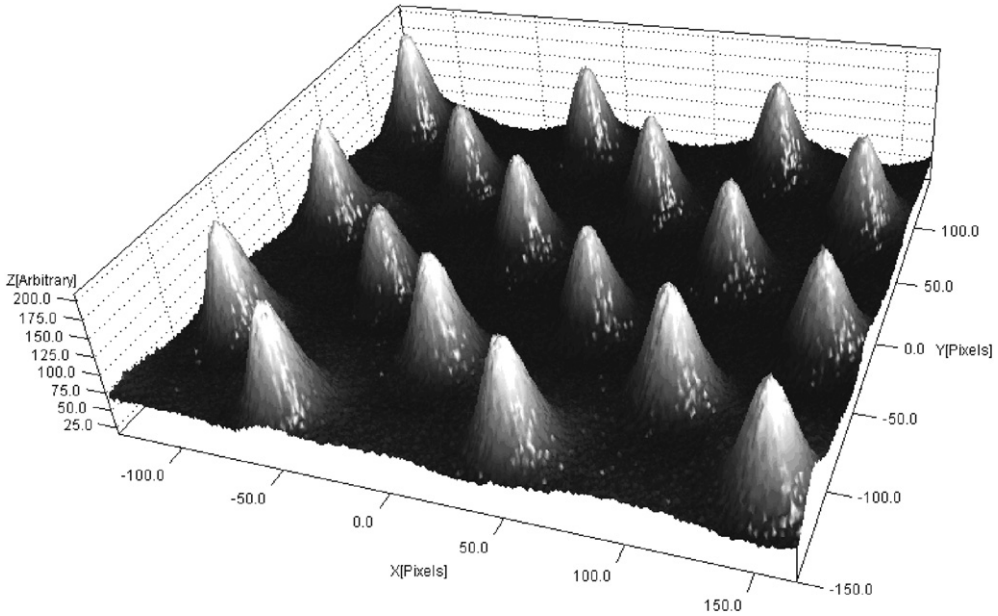

Figure 5. 3D rendering of TGT1 silicon grating (Carli *et al* 2010).

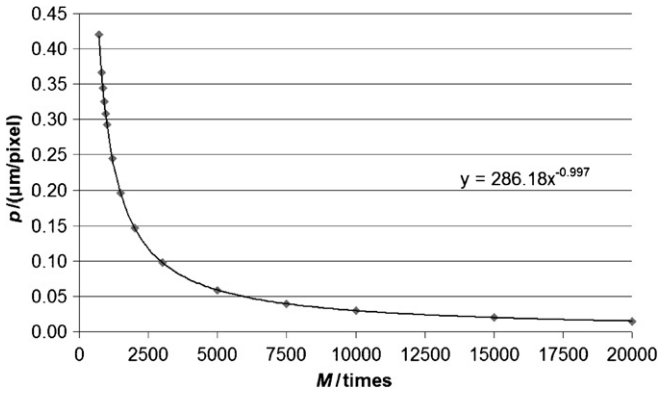

Figure 6. Empirical relation (regression dotted curve) between the pixel size p and magnification M calculated from 15 experiments.

magnification equal to 800×, that is near the lower bound of M in the measurement conditions, one half of the variability range equal to 1×10^{-3} μm/pixel can reasonably be assumed.

3.1.3. Resolution. The microscope spatial resolution indicated in the manufacturer's specifications is equal to 3 nm at 30 kV and 10 nm at 3 kV. Since the manufacturer performs resolution evaluation only for these two values, a linear trend of the SEM resolution as a function of the accelerating voltage has been assumed. In this way a resolution of 8.2 nm is obtained for an accelerating voltage of 10 kV, which has been used to acquire SEM images in this work.

3.2. Number of pixels

The same considerations apply to the numbers of pixels n_1 and n_2 relevant to coordinates y_1 and y_2, respectively.

3.2.1. Bias. Since the variable is a count, this contribution is not considered.

3.2.2. Reproducibility evaluation. The reproducibility in the identification of homologous points has been considered. It depends on the quality of the image and how the image is handled by the software. It is possible to evaluate the reproducibility for classes of images (well-defined details, visible details, blurry image). Rough values of reproducibility from 0.1 to 5 pixels were considered, based also on the available literature (Scharstein and Szeliski 2002).

3.2.3. Resolution. It is not considered, since it is contained in reproducibility.

3.3. Working distance

3.3.1. Bias evaluation. The calibration of the working distance d is problematic, since this quantity is not directly controllable. However this calibration can be omitted, as the contribution of the working distance in terms of overall uncertainty is negligible as will be demonstrated later on.

3.3.2. Reproducibility evaluation. In order to evaluate the reproducibility of the working distance d, its relation to the z-coordinate has been empirically derived. The z-axis was previously calibrated (Carli 2010) with reference to ISO 230-2:2006 (see figure 7).

Fixing main instrument settings (i.e. accelerating voltage, spot size and magnification), a total of 18 measurements of d were made along the lines of ISO 230-2:2006 (two backward and one forward series). The whole z-coordinate range has been explored in the measurement conditions (see figure 8).

The reproducibility of the working distance d can be assessed as deviation from a hypothetical model, that is the regression equation $d = az + b$. In particular, it has been

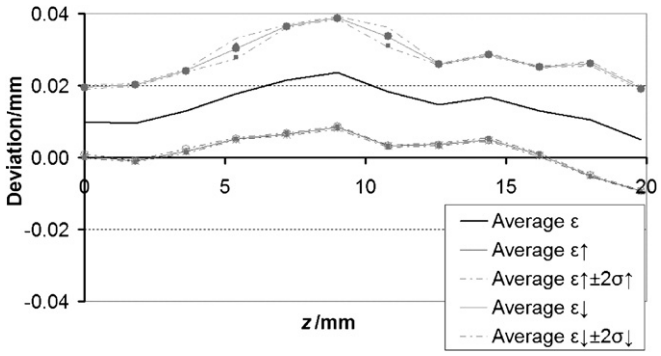

Figure 7. *Z*-axis bi-directional accuracy of positioning. Dark grey symbols represent runs taken while moving forwards, while light grey ones runs taken while moving backwards (Carli 2010).

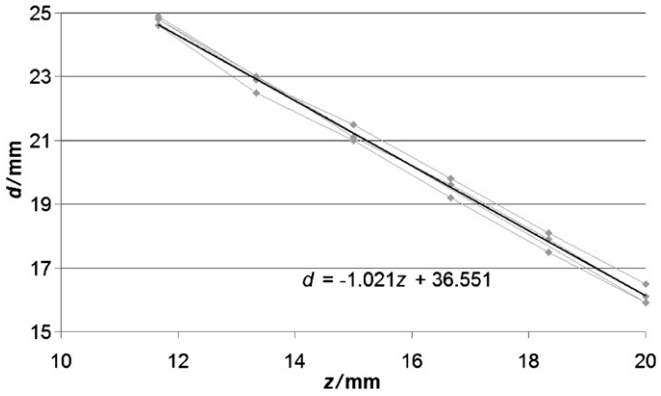

Figure 8. Empirical relation (regression line) between the working distance d and coordinate z (Genta 2010).

evaluated as standard deviation of regression residuals, which is equal to 0.25 mm.

Looking at the empirical relation (figure 8) an absolute value of slope different from unity implies that varying z (i.e. changing focus) also changes the focal length.

3.3.3. Resolution. The resolution is equal to 0.1 mm, as it can be read from the SEM controller. Since this value is lower than 50% of reproducibility, it can be neglected.

3.4. Rotational angle

The rotary table was calibrated for rotational angles φ between 0° and 360°.

3.4.1. Bias evaluation. The SPM calibration grating pitch, previously used for pixel size calibration, may also be adopted for calibration of the rotational angle φ. This calibration was performed along the lines of ISO 230-2:2006 (two forward and one backward series). The whole range of rotations of the rotary table was explored by carrying out a total of 93 measurements (see figure 9).

A systematic effect due to the resolution (sawtooth trend in figure 9) and one due to the characteristic of the rotary table

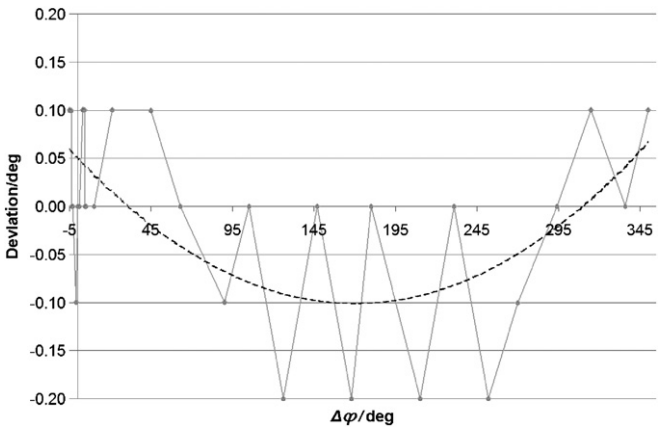

Figure 9. Rotational angle φ bi-directional accuracy of positioning. The deviation is modelled by a regression curve. Differences between run taken while moving forwards and backwards are negligible (Genta 2010).

may be observed, the deviation e of the latter being reasonably modelled by the parabola

$$e = a\varphi^2 + b\varphi + c, \tag{3}$$

where $a = 3.0 \times 10^{-4}$ rad^{-1}, $b = -1.8 \times 10^{-3}$ and $c = 8.7 \times 10^{-4}$ rad.

The systematic effect for any value of φ may thus be corrected. The parabolic correction is significant for the definition of the direction of view, while for the angle between two images is negligible against the variation given by the sawtooth effect.

In fact, in this case, assuming the stereo-pair angle $\Delta\varphi$ equal to 6.11×10^{-2} rad, the correction is found to be 9.8×10^{-4} rad in the worst case. When necessary, the uncertainty of model (3) can be considered, and approximated as

$$u_e^2 = (\varphi^2)^2 u_a^2 + \varphi^2 u_b^2 + u_c^2. \tag{4}$$

The terms u_a, u_b and u_c are known from regression, while $\Delta\varphi$ is the rotational angle adopted. Concluding, in the case at hand, the bias u_e to be considered is 0.011°, i.e. 2.0×10^{-4} rad.

As far as the sawtooth effect is concerned, a mathematical model may not be implemented owing to lack of information (the pattern in the interval between any couple of experimental points being unknown); therefore it is taken into account by the reproducibility evaluation.

3.4.2. Reproducibility evaluation. It can be evaluated as the standard deviation of regression residuals against parabolic pattern (see figure 9), which is equal to 0.077°, i.e. 1.3×10^{-3} rad.

3.4.3. Resolution. The resolution is equal to 0.1°, i.e. 1.7×10^{-3} rad. It has to be considered, since it is greater than reproducibility.

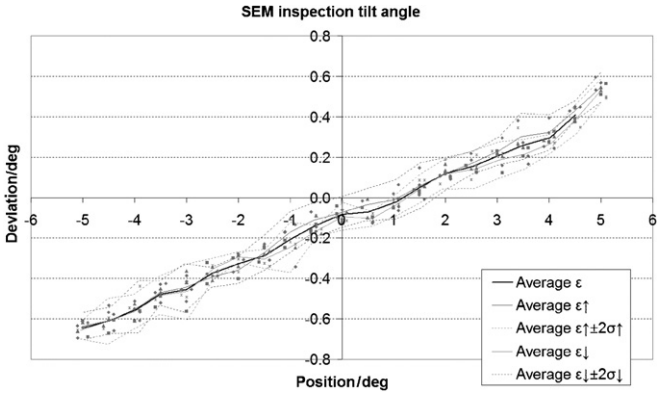

Figure 10. Tilt angle bi-directional accuracy of positioning. Dark grey symbols represent runs taken while moving forwards, while light grey ones runs taken while moving backwards (Carli 2010).

3.5. Tilt angle

3.5.1. Bias evaluation. The tilt angle φ was previously calibrated (Carli 2010) with reference to ISO 230-2:2006 (see figure 10).

As shown in figure 10, the deviation e is reasonably modelled by the regression line

$$e = a\varphi + b, \tag{5}$$

where $a = 1.1 \times 10^{-1}$ and $b = -1.9 \times 10^{-3}$ rad. The systematic effect for any value of φ may thus be corrected. The correction, more significant than the case of the rotational angle, can lead to a different management of model (2). The stereo-pair angle $\Delta\varphi$ can be represented by

$$\Delta\varphi = \frac{\varphi_{dx} - \varphi_{sx}}{2}, \tag{6}$$

where φ_{sx} is relevant to the first image (negative tilt angle), while φ_{dx} is relevant to the second image (positive tilt angle). These two angles can respectively be corrected by

$$\varphi_{sx} = \varphi_1 + a\varphi_1 + b \tag{7}$$

and

$$\varphi_{dx} = \varphi_2 + a\varphi_2 + b, \tag{8}$$

where φ_1 and φ_2 are the two angles that have been set.

In this way, the stereo-pair angle $\Delta\varphi$ can be modelled by

$$\Delta\varphi = \frac{\varphi_2 - \varphi_1 + a\,(\varphi_2 - \varphi_1)}{2}. \tag{9}$$

In the case under consideration, assuming φ_1 equal to -6.11×10^{-2} rad and φ_2 equal to 6.11×10^{-2} rad, the corrected angles φ_{sx} and φ_{dx} result to be respectively -6.97×10^{-2} and 6.60×10^{-2} rad. The correction is not the same because the model has an intercept. The corrected value of the stereo-pair angle $\Delta\varphi$ results to be 6.79×10^{-2} rad. Once the systematic effect has been corrected, the uncertainty of models (7) and (8) has to be considered. It is taken into account in terms of reproducibility.

The standard deviation of coefficient a, that is equal to 1.2×10^{-3}, has also to be taken into account. It is a bias contribution for both tilt angles φ_1 and φ_2 because it applies to both corrections.

3.5.2. Reproducibility evaluation. It can be evaluated as the uncertainty of models (7) and (8). In particular, for both tilt angles φ_1 and φ_2, the reproducibility can be assessed as the standard deviation of regression residuals against line (9), which is equal to 9.1×10^{-4} rad.

3.5.3. Resolution. The resolution is equal to 0.1°, i.e. 1.7×10^{-3} rad. It has to be considered, since it is greater than reproducibility for both tilt angles φ_1 and φ_2.

4. Uncertainty budget

The aim is to refer the uncertainty evaluation to the measurement of a wire gauge with nominal radius equal to 125 μm, already the subject of a previous analysis (Carli *et al* 2009).

Two possible movements of the rotary table have been considered, i.e. rotation and tilt. First of all, uncertainty evaluation through an uncertainty table is briefly described (section 4.1), and then uncertainty assessment is performed in the case of rotation (section 4.2) and tilt (section 4.3) of the rotary table.

4.1. The uncertainty table

The uncertainty evaluation according to GUM may be properly organized in a tabular format, as referred to EA-4/02:1999. A small modification from this format has been introduced by substituting standard deviations with variances; it has the advantage of managing additive quantities which can be compared more easily. In this way, the table shows individual contributions to the variance of the output quantity Y (Barbato *et al* 2005). Therefore, following the PUMA method (ISO 14253-2:1999), the most important uncertainty components clearly result (see tables 1 and 2).

Symbols of independent variables appearing in the mathematical model, their value and, if necessary, notes are written down in column x_j. Entries in column s_j are standard deviations for contributions of type A (GUM 4.2), and in column a_j one half of range for contributions of type B, as well as a k_a factor of 2, 3 or 6 respectively corresponding to a U-shaped, uniform or triangular distribution (GUM 4.3). Taking into account these considerations, for every contribution the variance $u^2(x_j)$ can be defined as s_j^2 (type A) or a_j^2 divided by the relevant k_a factor (type B). The coefficients of sensitivity may then be evaluated either by partial derivation, or numerically, and eventually contributions $u_j^2(y)$ of the variance of the dependent variable y can be calculated. The degrees of freedom (d.o.f.) ν_j of independent variables should be evaluated according to the following considerations (Barbato *et al* 2005):

- for type A contribution data numbers are known, and so are the relevant d.o.f.;
- for type B contribution information is usually fairly robust, and therefore the number of d.o.f. may be considered infinite (from a practical point of view 100 is large enough). The value of d.o.f. may also be taken as a figure of merit of the relevant variability information: if almost

Table 1. Uncertainty table in the case of rotation.

	x_j									
Symb.	Value	Note	s_j	a_j	k_{aj}	$u^2(x_j)$	c_j	$u_j^2(y)$	ν_j	$u_j^4(y)/\nu j$
p	2.93×10^{-7}	Bias		4.7×10^{-9}	3	7.3×10^{-18}	4.2×10^{2}	1.3×10^{-12}	30	5.8×10^{-26}
		Res.		4.1×10^{-9}	3	5.6×10^{-18}	4.2×10^{2}	1.0×10^{-12}	100	1.0×10^{-26}
		Repr.	6.2×10^{-10}			3.8×10^{-19}	4.2×10^{2}	6.9×10^{-14}	4	1.2×10^{-27}
n_1	4.26×10^{2}	Repr.		5.0×10^{-1}	3	8.3×10^{-2}	2.4×10^{-6}	4.7×10^{-13}	30	7.4×10^{-27}
n_2	3.75×10^{2}	Repr.		5.0×10^{-1}	3	8.3×10^{-2}	-2.4×10^{-6}	4.7×10^{-13}	30	7.3×10^{-27}
$\Delta\varphi$	6.01×10^{-2}	Bias	2.0×10^{-4}			3.9×10^{-8}	-2.0×10^{-3}	1.6×10^{-13}	90	2.8×10^{-28}
		Res.		8.7×10^{-4}	3	2.5×10^{-7}	-2.0×10^{-3}	1.0×10^{-12}	100	1.0×10^{-26}
		Repr.	1.3×10^{-3}			1.8×10^{-6}	-2.0×10^{-3}	7.2×10^{-12}	90	5.8×10^{-25}
d	8.60×10^{-3}	Repr.	2.5×10^{-4}			6.2×10^{-8}	2.8×10^{-5}	4.9×10^{-17}	16	1.5×10^{-34}
z	1.25×10^{-4}							1.2×10^{-11}	Σ	6.7×10^{-25}
						Standard deviation of $y(z)$		3.4×10^{-6}	ν_y	204
						Confidence level		95%		
						Coverage factor		2.0		
						Expanded uncertainty		6.7×10^{-6}		

Table 2. Uncertainty table in the case of tilt.

	x_j									
Symb.	Value	Note	s_j	a_j	k_{aj}	$u^2(x_j)$	c_j	$u_j^2(y)$	ν_j	$u_j^4(y)/\nu j$
p	3.66×10^{-7}	Bias		5.9×10^{-9}	3	1.1×10^{-17}	3.4×10^{2}	1.3×10^{-12}	30	5.9×10^{-26}
		Res.		4.1×10^{-9}	3	5.6×10^{-18}	3.4×10^{2}	6.5×10^{-13}	100	4.3×10^{-27}
		Repr.		1.0×10^{-9}	3	3.3×10^{-19}	3.4×10^{2}	3.9×10^{-14}	30	5.0×10^{-29}
n_1	3.41×10^{2}	Repr.		5.0×10^{-1}	3	8.3×10^{-2}	2.7×10^{-6}	5.9×10^{-13}	30	1.2×10^{-26}
n_2	2.95×10^{2}	Repr.		5.0×10^{-1}	3	8.3×10^{-2}	-2.7×10^{-6}	5.9×10^{-13}	30	1.2×10^{-26}
φ_1	-6.11×10^{-2}	Res		8.7×10^{-4}	3	2.5×10^{-7}	1.0×10^{-3}	2.6×10^{-13}	100	6.7×10^{-28}
		Repr.	9.1×10^{-4}			8.3×10^{-7}	1.0×10^{-3}	8.5×10^{-13}	100	7.1×10^{-27}
a_1	1.1×10^{-1}	Bias	1.2×10^{-3}			1.4×10^{-6}	-5.5×10^{-5}	4.3×10^{-15}	100	1.8×10^{-31}
φ_2	6.11×10^{-2}	Res		8.7×10^{-4}	3	2.5×10^{-7}	-1.0×10^{-3}	2.6×10^{-13}	100	6.5×10^{-28}
		Repr.	9.1×10^{-4}			8.3×10^{-7}	-1.0×10^{-3}	8.3×10^{-13}	100	6.9×10^{-27}
a_2	1.1×10^{-1}	Bias	1.2×10^{-3}			1.4×10^{-6}	-5.5×10^{-5}	4.3×10^{-15}	100	1.8×10^{-31}
d	1.60×10^{-2}	Repr.	2.5×10^{-4}			6.2×10^{-8}	8.6×10^{-6}	4.6×10^{-18}	16	1.3×10^{-36}
z	1.25×10^{-4}							5.4×10^{-12}	Σ	1.0×10^{-25}
						Standard deviation of $y(z)$		2.3×10^{-6}	ν_y	286
						Confidence level		95%		
						Coverage factor		2.0		
						Expanded uncertainty		4.6×10^{-6}		

certain one can take e.g. 100 d.o.f., if it is of medium level one can put 30 d.o.f., if of low level 15 d.o.f. or less.

Further details are given in Genta (2010).

4.2. *Uncertainty in the case of rotation*

The expected values of independent variables are theoretically evaluated in the measurement conditions.

The rotational angle $\Delta\varphi$ is *a priori* set, based on past experience (Carli *et al* 2009); in this case $\Delta\varphi$ is assumed equal to 3.5°, i.e. 6.11×10^{-2} rad. The value of the working distance d is read on the SEM screen during the measurement; it is closely related to the measurand dimension and set level of magnification. In the case at hand, for magnification equal to 1000×, the working distance is 8.6 mm, while the pixel size is 0.293 μm/pixel.

Referring to a point on the surface of the wire gauge, considered as an ideal cylinder, it is assumed that $y_1 = 125\ \mu$m. Looking at figure 4, it is noticeable that y_2 depends on the vertical elevation z; therefore, by inverting the first relation of (1), the coordinate y_2 can be expressed as a function of the input variables y_1, d, $\Delta\varphi$ and the output variable z as

$$y_2 = \frac{d^2 z \sin(2\Delta\varphi) - d^2 y_1 \cos(\Delta\varphi) + dz y_1 \cos(2\Delta\varphi)}{-d^2 \cos(\Delta\varphi) + dz \cos(2\Delta\varphi) + 2dy_1 \sin(\Delta\varphi) - z y_1 \sin(2\Delta\varphi)}. \quad (10)$$

For the adopted operational conditions, the coordinate y_2 results equal to about 110 μm. Finally, the numbers of pixels $n_1 \approx 426$ and $n_2 \approx 375$ are immediately derived from y_1 and y_2, respectively.

Referring to these preliminary considerations and to the detailed description of uncertainty contributions given in the previous section, the preparation of table 1 is straightforward. SI units are adopted, without any multiples or submultiples.

The calculation of sensitivity coefficients is difficult; therefore these are numerically approximated. A detailed analysis of sensitivity coefficients has been performed in

Table 3. Percentage influences on $U(z)$, the value of $U(z)$ and value of $U(z)/z$, varying reproducibility of n_1 and n_2, in the case of rotation.

Repr. n_1 and n_2 (pixel)	Percentage influence on $U(z)$			$U(z)$ (m)	$U(z)/z$ (%)
	p	n_1 and n_2	$\Delta\varphi$		
0.1	22	0	78	6.5×10^{-6}	5.2
0.5	22	2	76	6.5×10^{-6}	5.3
1	20	8	72	6.7×10^{-6}	5.4
5	7	68	25	1.2×10^{-5}	9.3

Bariani (2005), to which reference is made to validate numerical approximations.

The expanded uncertainty on the vertical elevation z results to be equal to 6.7 μm.

4.3. Uncertainty in the case of tilt

The tilt angle $\Delta\varphi$ is set equal to 3.5°, that is 6.11×10^{-2} rad, similar to the rotational angle. Model (9) for the stereo-pair angle $\Delta\varphi$ is directly inserted in (2). In the measurement conditions, the magnification level is equal to 800×; therefore the pixel size is 0.366 μm/pixel. The value of the working distance d, read on the SEM screen, results to be 16.0 mm.

Referring to a point on the surface of the wire gauge, it is again assumed $y_1 = 125$ μm, and therefore, through (10), the coordinate y_2 results to be equal to about 108 μm. Finally, the numbers of pixels $n_1 \approx 341$ and $n_2 \approx 295$ are immediately derived.

The expanded uncertainty on the vertical elevation z results to be equal to 4.6 μm.

5. Discussion

As previously mentioned, regarding the reproducibility evaluation of the number of pixels, it is possible to make an uncertainty assessment for classes of images, associating their quality with the reproducibility in the identification of homologous points. Tables 3 and 4 indicate the percentages of influence of each contribution on the expanded uncertainty $U(z)$, value of $U(z)$ and value of relative expanded uncertainty $U(z)/z$, varying reproducibility of n_1 and n_2 from 0.1 to 5 pixels, in the case of rotation and tilt. The contribution of the working distance d is omitted because it is always negligible.

Figure 11 shows the trends of percentage influence on $U(z)$ of n_1 and n_2 with the increase of their reproducibility in the case of rotation and tilt, while figure 12 reports the trends of relative expanded uncertainty $U(z)/z$.

For a certain value of reproducibility of n_1 and n_2, in the case of rotation a lower percentage influence on $U(z)$ (figure 11) and a higher value of relative expanded uncertainty $U(z)/z$ (figure 12) are noticed. This is due to the fact that the systematic error (sawtooth trend) has not been corrected in the case of rotation.

Table 4. Percentage influences on $U(z)$, the value of $U(z)$ and value of $U(z)/z$, varying reproducibility of n_1 and n_2, in the case of tilt.

Repr. n_1 and n_2 (pixel)	Percentage influence on $U(z)$			$U(z)$ (m)	$U(z)/z$ (%)
	p	n_1 and n_2	$\Delta\varphi$		
0.1	48	0	52	4.1×10^{-6}	3.2
0.5	45	7	49	4.2×10^{-6}	3.3
1	37	22	41	4.6×10^{-6}	3.7
5	6	87	7	1.2×10^{-5}	9.2

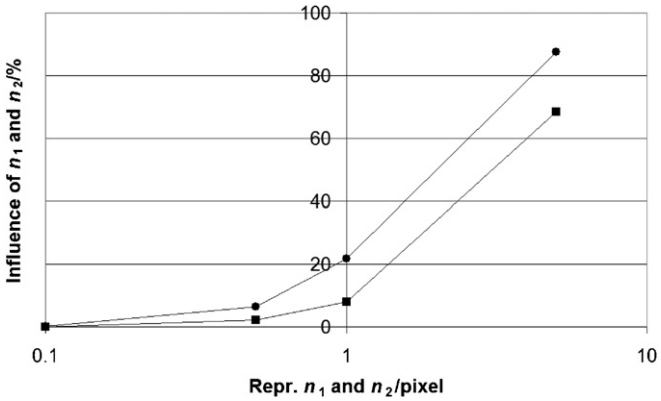

Figure 11. Trends of percentage influence on $U(z)$ of n_1 and n_2 with the increase of their reproducibility in the case of rotation (squares) and tilt (circles).

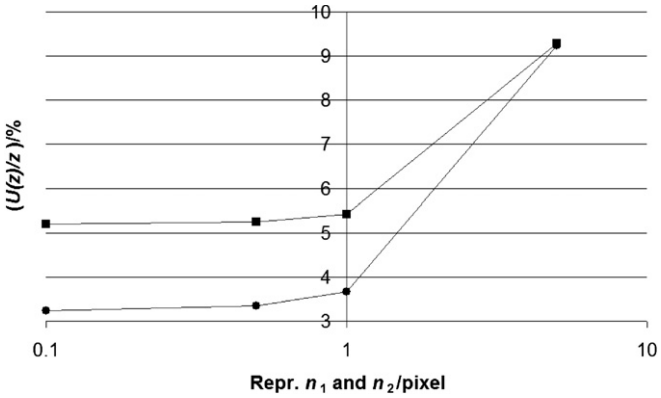

Figure 12. Trends of relative expanded uncertainty $U(z)/z$ with the increase of reproducibility of n_1 and n_2 in the case of rotation (squares) and tilt (circles).

Basing on experimental evidence, a value of 1 pixel has been chosen as typical reproducibility. For the case of rotations, examining table 1, the largest contribution is due to the reproducibility of the rotational angle $\Delta\varphi$, followed by the bias of the pixel size p. Therefore, in order to reduce the uncertainty in 3D-SEM reconstructions, performances of the rotary table should be above all improved. As the main contribution in rotational angle reproducibility is due to the sawtooth trend, a more refined calibration is needed, in order to produce a correction table. Thereafter, one can check whether the parabolic correction of the φ bias reaches significance. Moreover, after these corrections, the contribution of the

p bias may rise near the first place, therefore dictating a better calibration of the artefact.

For the case of tilting, with reference to table 2, the largest contribution is due to the bias of the pixel size p, followed by the reproducibility of the tilt angle $\Delta\varphi$. Therefore, in order to reduce the uncertainty in 3D-SEM reconstructions when performing tilting, a calibrated artefact, with a lower uncertainty, should be adopted to refine pixel size bias calculation. Moreover, the high uncertainty associated with tilt reproducibility, is due to the fact that the stage can be tilted only manually by the operator, while, for instance, rotations are controlled by the piezo-motor of the stage. Therefore, since this uncertainty contribution cannot be improved by further calibrations, another positioning system allowing item tilting should be adopted to improve the performances.

6. Conclusions

A theoretical uncertainty evaluation of the stereo-pair technique, according to GUM (JCGM 100:2008), was carried out. As a case study, 3D-SEM reconstructions, performed on a wire gauge with a reference diameter of 250 μm, were considered. Starting from the most commonly used tilting strategy, performed to obtain images composing the stereo-pair, a multi-view strategy through item rotation was also considered for the uncertainty evaluation. This methodology allows obtaining 3D reconstructions of the complete geometry of the cylindrical item, by acquiring SEM images rotating the item along its main axis. The theoretical uncertainty evaluation was performed starting from a modified version of the Piazzesi equation, enabling the calculation of the z-coordinate from a given stereo-pair. The pixel size p, the number of pixels n_1 and n_2, the working distance d and the tilt (or rotation) angle $\Delta\varphi$ were considered as independent variables. The metrological characteristics of each input variable (p, n_1, n_2, d and $\Delta\varphi$) were taken into account, and the uncertainty, in terms of bias, resolution and reproducibility for each variable, was calculated. An uncertainty table for the case of tilt and rotation was then produced leading to the calculation of the final expanded uncertainty value. The main conclusions of this theoretical uncertainty evaluation were the following.

- For the case of *rotations*, the largest uncertainty contribution is due to the reproducibility of the rotational angle $\Delta\varphi$, followed by the bias of the pixel size p. Therefore, in order to reduce the uncertainty in 3D-SEM reconstructions, performances of the rotary table should be improved and/or a different calibration procedure could be, for instance, considered by employing a different artefact.
- For the case of *tilting*, the largest uncertainty contribution is due to the bias of the pixel size p, followed by the reproducibility of the tilt angle $\Delta\varphi$. Therefore, in order to reduce the uncertainty in 3D-SEM reconstructions when performing tilting, a calibrated artefact, with a lower uncertainty, should be adopted to refine pixel size bias calculation. Moreover, the high uncertainty associated with tilt reproducibility is due to the fact that the stage can be tilted only manually by the operator. Therefore, since this uncertainty contribution cannot be improved by further calibrations, another positioning system allowing item tilting should be adopted to improve the performances.
- An expanded uncertainty equal to 6.7 μm was calculated in the case of item rotation (table 1), while it was calculated to be equal to 4.6 μm in the case of tilting (table 2), where a correction of the systematic error due to stage tilting was performed. Comparing the expanded uncertainties, obtained from the theoretical uncertainty evaluation, with the cylindrical item radius of 125 μm, it can be concluded that a 5.4% and a 3.7% relative expanded uncertainty is obtained in the case of rotation and tilt respectively.

References

Barbato G, Germak A and D'Agostino D 2005 *Misurare Per Decidere* (Bologna: Progetto Leonardo) (in Italian)

Bariani P 2005 Dimensional metrology for microtechnology *PhD Thesis* IPL DTU, Kongens Lyngby, Denmark

Bariani P, De Chiffre L, Hansen H N and Horsewell A 2005 Investigation on the traceability of three-dimensional scanning electron microscope measurements based on the stereo-pair technique *Precis. Eng.* **29** 219–28

Boyde A 1973 Quantitative photogrammetric analysis and qualitative stereoscopic analysis of SEM images *J. Microsc.* **98** 452–71

Carli L 2010 3D-SEM metrology for coordinate measurements at the nanometer scale *PhD Thesis* Department of Mechanical Engineering DTU, Kongens Lyngby, Denmark

Carli L, De Chiffre L, Horsewell A, Carmignato S, Caroli M and Santin D 2009 Improvement of geometrical measurements from 3D-SEM reconstructions *Proc. 11th CIRP Int. Conf. on Computer Aided Tolerancing* pp 1–7

Carli L, Genta G, Cantatore A, Barbato G, De Chiffre L and Levi R 2010 Experimental investigation on the influence of instrument settings on pixel size and nonlinearity in SEM image formation *Proc. 10th EUSPEN Int. Conf.* pp 192–5

EA 1999 Expressions of the uncertainty of measurements in calibration EA-4/02:1999, European Co-operation for Accreditation

Genta G 2010 *Methods for Uncertainty Evaluation in Measurement* (Saarbrücken: VDM Verlag)

Goodhew P, Humphreys J and Beanland R 2001 *Electron Microscopy and Analysis* 3rd edn (London: Taylor and Francis)

Hillmann W 1980 Rauheitsmessung mit dem Raster–Elektronenmikroskop (REM) *Tech. Mess. tm* **9116** 6 (in German)

ISO 1999 Geometrical product specifications (GPS)—inspection by measurement of workpieces and measuring equipment—part 2. Guide to the estimation of uncertainty in GPS measurement, in calibration of measuring equipment and in product verification ISO 14253-2:1999, International Organization for Standardization

ISO 2006 Test code for machine tools—part 2. Determination of accuracy and repeatability of positioning numerically controlled axes ISO 230-2:2006, International Organization for Standardization

ISO/IEC 2005 General requirements for the competence of testing and calibration laboratories ISO/IEC 17025:2005, International Organization for Standardization

JCGM (Joint Committee for Guides in Metrology) 2008 *Evaluation of Measurement Data—Guide to the Expression of Uncertainty in Measurement (GUM)*, JCGM 100:2008

JCGM (Joint Committee for Guides in Metrology) 2008 *International Vocabulary of Metrology—Basic and General Concepts and Associated Terms (VIM)*, JCGM 200:2008

Kolednik O 1981 A contribution to stereo-photogrammetry with the scanning electron microscope *Prakt. Metallogr.* **18** 562–73

Marinello F, Bariani P, Savio E, Horsewell A and De Chiffre L 2008b Critical factors in SEM 3D stereo microscopy *Meas. Sci. Technol.* **19** 065705

Marinello F, Carmignato S, Savio E, Bariani P, Carli L, Horsewell A and De Chiffre L 2008a Metrological performance of SEM 3D techniques *Proc. 18th IMEKO TC 2 Symp. on Photonics in Measurements* pp 1–6

Piazzesi G 1973 Photogrammetry with the scanning electron microscope *J. Phys. E: Sci. Instrum.* **6** 392–6

Sato H 1990 A way to measurement for submicron meter: surface profile by scanning electron microscope *Proc. Manufacturing International* pp 63–73

Scharstein D and Szeliski R 2002 A taxonomy and evaluation of dense two-frame stereo correspondence algorithms *Int. J. Comput. Vision.* **47** 7–42

Scherer S 2002 3D surface analysis in scanning electron microscopy *G.I.T. Imaging and Microscopy* **3** 45–6

Schubert M, Gleichmann A, Hemmleb M, Albertz J and Köhler J M 1996 Determination of the height of a microstructure sample by a SEM with a conventional and a digital photogrammetric method *Ultramicroscopy* **63** 57–64